

# Analysis of a Sample of RC Catalog Objects in the Region Overlapping with the Areas Covered by FIRST and SDSS Surveys. II: Optical Identification with the SDSS Survey and USNO-B1 and 2MASS Catalogs

O. P. Zhelenkova<sup>1</sup> and A. I. Kopylov<sup>1</sup>

<sup>1</sup>*Special Astrophysical Observatory of the Russian AS, Nizhnij Arkhyz 369167, Russia*

We report the results of optical identification of a sample of RC catalog radio sources with the FIRST and SDSS surveys. For 320 sources identified with NVSS and FIRST objects we perform optical identification with the SDSS survey. When selecting optical candidates we make maximum use of the information about the structure of radio sources as provided by the FIRST survey images. We find optical candidates for about 80% of all radio sources.

## 1. INTRODUCTION

Powerful radio galaxies can be observed almost at any cosmological distance, however, their host galaxies are often optically faint. Much observational time is needed to identify a radio source and find the redshift of its host galaxy. The history of the identification of the 3CR catalog of bright radio sources ( $\nu=187$  MHz,  $S_{lim}=5$  Jy) [1, 2] serves to illustrate this point. The limiting magnitude of the Palomar Observatory Sky Survey (POSS) of about  $20.5^m$  for E plates, proved to be sufficient to allow the identification of 65% of all radio sources of the catalog, whereas it took almost three decades to identify the remaining 35% [3–8]. The number of optically identified radio sources rapidly decreases at lower fluxes. For example, the fraction of POSS identifications for B2 survey ( $\nu=408$  MHz,  $S_{lim} = 250$  mJy) is equal to 38% [9], whereas the corresponding fraction for deeper the First ( $\nu= 610$  MHz,  $S_{lim} \sim 20$ mJy) and the Second

( $\nu=1415$  MHz,  $S_{lim} \sim 7$ mJy) Westerbork surveys is even lower, of about 20% [10].

The field of view of a large telescope does not exceed  $10' - 20'$ , making the task of finding enough reference stars for the astrometric calibration problematic at the times before the release of the APM [11], USNO [12], and GSC [13] catalogs. For this reason, secondary astrometric standards had to be used in the fields studied.

Extended radio sources with complex structure are identified using composite images made up of optical and radio frames. A reliable choice of the optical candidate requires accurate coordinate calibration (to within  $1''$ ), high-resolution radio images (e.g., like those of the FIRST survey with an angular resolution of  $5.4''$ ), and deep direct optical images (with an R-band limiting magnitude of  $23^m-24.5^m$ ) with the astrometric calibration accuracy at least as good as that of the radio image. If even after this procedure there remain several optical candidates, additional information, e.g., broad-band photometry,

can be used to pick up the right one. However, only spectroscopic observations allow the host galaxy of the radio source to be reliably identified.

In early 1980s a deep survey was carried out with the RATAN-600 within a  $20'$ -wide sky strip centered at the declination of SS433 ( $\delta_{1950.0} = +4^{\circ}54'$ ). The survey angular resolution at 3.94 GHz ( $\lambda=7.6$  cm) was equal to  $\Delta\alpha \sim 1'$ . The RC catalog compiled based on the observation data of this survey has a coordinate accuracy of  $5'' \times 45''$  in right ascension and declination, respectively [14, 15]. The faintest sources detected have flux densities of about 4 mJy. The completeness of the catalog is equal to 0.8 for sources with flux densities  $S_{3.94\text{GHz}} > 7.5$  mJy within the  $\pm 5'$  strip about the central declination of the survey. The RC catalog contains a total of 1165 sources [16, 17].

A pilot program of optical identification of objects of the RC catalog was performed using the photographic data obtained in 1984–1989 with the 6-m telescope of the Special Astrophysical Observatory of the Russian Academy of Sciences [18]. It was followed by the identification of a 266-object sample with the refined coordinates based on the TXS catalog [19] via inspection of enlarged POSS prints [20, 21]. Optical candidates have been found for 72 ( $\sim 27\%$ ) of these objects.

The next stage of the work involved the identification of a sample of steep-spectrum radio sources of the RC catalog on deep CCD im-

ages ( $m_R^{lim} \sim 24^m$ ) taken with the 6-m telescope within the framework of the “Big Trio” program of the search for distant radio galaxies [22–24]. The astrometric calibration of small regions of CCD frames (about  $3' \times 3'$ ) was based on secondary standards whose coordinates were determined using POSS-I images [25] and APM and GSC catalogs. Identification was performed by means of overlapping high-resolution VLA radio images with optical images.

The release of the deep optical SDSS sky survey [26] and the FIRST radio survey [27] made it possible to continue the identification of RC objects and refine the results of the identification of radio sources performed by Soboleva et al. [20] and Fletcher et al. [21]. About 50% of FIRST radio sources are estimated to be identified down to the limiting magnitude of the SDSS survey ( $m_r = 22.6^m$ ), and we therefore believed that at least the same fraction of RC objects can be identified with SDSS.

## 2. OPTICAL IDENTIFICATION

The RC catalog overlaps with the SDSS and FIRST surveys in the right-ascension interval from  $8^h11^m$  to  $16^h25^m$ , which includes a total of 432 objects. A comparison of the images of the NVSS survey [28] with angular resolution of  $45''$  with the FIRST survey images with an angular resolution of  $5.4''$  shows that the latter should be used for optical identification, especially in cases where the corresponding NVSS object is

not a point source (angular size exceeds  $23''$ ) and breaks into independent sources in the FIRST images.

In complex cases (multicomponent sources, groups of independent radio sources, or several optical candidates) detailed information about the structure of the source is required for optical identification. To establish the structure of the radio sources according to the FIRST survey data in more detail, we not only drew the contours using the Aladin application [29], but also employed a software tool that draws flux density isophotes in the areas studied without the loss of angular resolution [30].

The structure of the radio source correlates with the position of the host galaxy, and therefore not only on the coordinate coincidence, but also on the morphological type of the source should be taken into account when choosing the optical candidate. We based our morphological classification of radio sources on a slightly modified variant of the scheme proposed by Lawrence et al. [31]. Our classification includes the following types:

- point radio sources (core or C). The positions of their host galaxies most likely coincide with the flux density peak;
- sources with one-sided jets (core-jet or CJ). For such sources, the position of the optical candidate coincides with that of the bright compact component;
- sources with a bright core and components

(core-lobe or CL). In these sources intensity of radio emission decreases from the center toward the periphery. The optical candidate coincides with the peak of the intensity distribution;

- double sources (double or D) and double sources with double components (double-double or DD). The optical candidate in double radio sources is located between the components or coincides with the minimum of the intensity distribution between the merging components;
- double sources with a core (double-core or DC). A double source with a faint core located between the components. The optical candidate coincides with the core;
- triple sources (T). The radio source consists of three components, where the flux of the central part is comparable to those of the other two components. The optical candidate coincides with the central component;
- multiple sources (M). These are multicomponent sources with a structure that is difficult to put into any of the above categories. In this case the position of the optical candidate is not easy to determine and additional photometric or spectroscopic information is needed for a choice of the optical objects located within the error box of the coordinate calibration.

We classified 320 sources in accordance with this scheme. We then determined the position of the optical candidate based on the morphological type of the source. In a number of cases its position with respect to the isophotes of the radio image made it possible to refine the type of the radio source or identify the components with individual radio sources. For example, if each of the components of the presumed double source had the size of about  $2''$  and coincided with a certain optical object, we regarded it as two point sources, because accidental coincidence is highly unlikely due to the low surface density of the radio sources.

We took the following coordinates for a intended optical candidate (hereafter referred to as the center of the radio source):

- F—the coordinates of the point source or of the source with a well-defined core as listed in the FIRST catalog (213 sources);
- N—if the source has two components with different flux densities in the FIRST survey, which constitute a single object in the NVSS, we adopt the NVSS coordinates, which correspond to the location of the center of mass the radio source, as the position of the optical object (32 sources);
- Fm—the coordinates of the center of the double source as measured by the contour map of the image in the FIRST survey (75 sources) in the following cases:

- (1) if the image contains a faint core with coordinates that are not listed in the FIRST catalog,
- (2) in the absence of a core the presumed position is determined by the contours of the FIRST radio image.

We consider the optical object to be the most likely candidate for identification (“+”) if it was located (according to the SDSS catalog) within  $3\sigma$  of the center of the radio source, where  $\sigma$  is the coordinate error. We consider identifications to be doubtful (“?”) in the following cases:

- if the object is a point source and the possible optical counterpart, albeit close, lies beyond  $3\sigma$  from the center of the radio source;
- if there are two optical objects in the vicinity of the expected location of the optical candidate;
- if the source is double, the position of its core is uncertain, and the optical object is offset from the line connecting the brightness maxima of the lobes;
- if it is difficult to make any definitive conclusions about the structure of the radio source based on the FIRST radio map (whether it should be viewed as a multicomponent radio source or several independent radio sources).

The average coordinate error of the FIRST survey is  $0.5''$ , amounting to  $1''$  for  $S_{1.4GHz} \sim$

1mJy sources. The accuracy of the radio coordinates is better than  $1''$  for NVSS survey sources with flux densities  $S_{1.4GHz} > 15$  mJy. We estimate the coordinate accuracy for the objects with the central part of the radio source identified using method “Fm” or “N” to be  $1''$ , and that for the objects with the central part of the radio source identified using method “F” to be  $0.5''$ . In the sky area studied the average density of SDSS objects (for  $m_r^{lim} = 22.6^m$ ) is about  $0.0020/\square''$ . The accuracy of the coordinate calibration of SDSS is about  $0.1''$ .

We use these values to compute the normalized distance  $D$  between the optical candidate and the center of the radio source:

$$D = \sqrt{\frac{\Delta\alpha^2}{\sigma_\alpha^2} + \frac{\Delta\delta^2}{\sigma_\delta^2}}, \text{ where } \sigma_\alpha^2 = \sigma_{\alpha_{rad}}^2 + \sigma_{\alpha_{opt}}^2$$

and  $\sigma_\delta^2 = \sigma_{\delta_{rad}}^2 + \sigma_{\delta_{opt}}^2$ .

We use the maximum-likelihood ratio  $LR^1$  as the effective estimate for the reliability of identification. We compute  $LR$  for point sources by the following formula:

$$LR(D) = \frac{1}{2\lambda} e^{\frac{D^2}{2}(2\lambda-1)}, \text{ where } \lambda = \pi\sigma_\alpha\sigma_\delta\rho$$

and  $\rho$  is the number of objects per square arcsecond.

The above formula can be used to compute  $LR$  if the position of the host galaxy can be reliably found from the structure of the radio source,

which is the case for the CJ, CL, DC, and T types described above (65% of all sources in our sample). We also use this formula to compute the  $LR$  values for double radio sources in the cases where the supposed position of the core can be reliably determined from the structure of the components. This is true for almost 2/3 of all double sources in our sample.

An empirical relation between the reliability and completeness of identification for radio sources [32] as a function of  $LR$  determines the cutoff value ( $LR_{cutoff}$ ), which separates identification from eventual chance coincidence with background objects.

The radio sources for which the optical candidates have been found can be subdivided into the following three groups by the morphological type and center of the radio source:

- point sources (C),
- sources where the peak of radio emission coincides with the optical object (CL, CJ, DC, and T), and
- double radio sources (D and DD), where the supposed position of the optical object was determined based on the shape of the isophotes of the radio image and not by the coordinates listed in the FIRST catalog.

The cutoff levels of the maximum-likelihood ratios,  $LR_{cutoff}$ , and the corresponding offsets  $d_{rad-opt}$  between the optical and radio coordinates proved to be more or less the same for all

---

<sup>1</sup> See [32] for a detailed description of the procedure employed to compute the probability, reliability, and completeness of optical identification for point and double radio sources. We adopted the above formulae from that paper.

the three groups (see Table 1), thereby lending a certain support to our proposed procedure of searching for optical candidates.

We use the computed  $LR$  ratios for the optical candidates and the  $LR_{cutoff}$  values as a testing criterion in the selection of the most likely identification. Figure 1 shows the distribution of the offsets between the radio and optical coordinates for the “+” and “?” optical candidates.

There are gaps in the equatorial area of the SDSS survey. Inside these gaps we searched for optical candidates of radio sources in the USNO-B1 catalog and identified one source (RC J1623+0446) in such a way.

We found another source (RC J1052+0458) to have an optical candidate in the SDSS images, but lack the data in the SDSS database. This object is listed in the USNO-B1 ( $R2 = 19.45^m$ ) and 2MASS catalogs [33] ( $K = 14.99^m$ ).

Below we give a few examples of the identification of radio sources and the reasoning used to select the optical candidates.

We found two optical candidates for the RC J1257+0458 source: a galaxy (SDSS type “GALAXY”) and a starlike object (“STAR”). By its u, g, r, i, and z-band magnitudes the latter looks more like a star rather than a quasar (quasars, too, are classified as “STAR”). We chose the galaxy as the optical candidate.

In the first our paper [34] dedicated to the identification of the RC catalog with the VLSS, TXS, NVSS, FIRST, and GB6 radio catalogs we give an identification for the double radio source

RC J0815+0453. It is evident from the radio isophotes that RC J0815+0453 has a well-defined core, which exactly coincides with the galaxy and hence the latter is the true optical identification rather than the fainter object located precisely on the line connecting the intensity maxima of the radio source lobes. There is yet another faint FIRST J081521.3+045339 radio source ( $S_{1.4GHz}^{peak} = 2.67$  mJy) near RC J0815+0453. Both radio sources are identified with elliptical galaxies with practically the same photometric redshifts. Thus, according to SDSS data, the photometric redshift of the host galaxy of the fainter radio source is  $Z_{phot1} = 0.0933 \pm 0.0049$  (based on the approximation by pattern spectra [35]) and  $Z_{phot2} = 0.0697 \pm 0.0142$  (neural-network method [36]). The corresponding photometric redshift estimates for the second galaxy are  $Z_{phot1} = 0.1235 \pm 0.0052$  and  $Z_{phot2} = 0.0694 \pm 0.0149$ , respectively. It seems fair to suppose—although this requires further studies—that the two sources form a close, possibly an interacting, pair of radio galaxies.

The identification of RC J0916+0441 required a detailed information on its structure. Thus one might conclude, based on the isophotes of the FIRST survey image produced by Aladin application, that RC J0916+0441 should be a blend of two independent radio sources—the Northern source consisting of two objects of the FIRST catalog and the Southern source consisting of four sources of the FIRST catalog. However, the isophotes drawn with angular resolution pre-

served (we use the software service [30] to this end) allowed us to understand the structure of the source. It proved to be an object of morphological type “core-lobe” with the core coincident with a galaxy (see Fig. 2).

We show our next example in Fig. 3. Here RC J0952+0453 is located between the components of a double NVSS source, closer to the brighter component. It is evident from the shape of their isophotes as shown on the FIRST contour map that the source components are unconnected, their orientation is not coaxial, and each component can be identified with a separate optical object. The RC J0952+0453 source is thus a blend of two independent radio sources.

In similar cases, where the size of the beam of RATAN-600 does not make it possible to resolve close radio sources, we assumed the brightest component to be the main contributor to the RC catalog source and then proceeded to its optical identification.

### 3. RESULTS OF IDENTIFICATION

In our first paper [34] we identified 320 of a total of 432 sources of the RC catalog located inside the area of intersection of the SDSS and FIRST surveys. A visual inspection of SDSS images superimposed on FIRST contour maps using refined coordinates allowed us to find bonafide (“+”) optical candidates for 227 (71%) of the radio sources; likely (“?”) optical candidates for 25 (8%) of the radio sources, with no optical

candidates to be found for 68 (21%) of all radio sources.

The area considered contains 36 objects of the sample of RC sources with steep spectra (SS). We earlier identified 35 sources using the 6-m telescope CCD images within the framework of the “Big Trio” program. For 10 of these objects we found no optical candidates in the SDSS survey.

Optical candidates (“+” and “?”) were found for 264 (82%) radio sources out of 320 objects. These include the SS sample and MG J1131+0456<sup>2</sup>. Note that the summary statistical data below does not include the 11 objects identified using deeper images.

Of all the radio sources identified with SDSS, 89 are stellar objects (“STAR”), 158 are galaxies (“GALAXY”), and six faint objects are classified as “UNKNOWN” in the SDSS database. Stellar objects are generally brighter (see Fig. 4) and bluer than galaxies.

Table 2 lists the results of identification of radio sources for different types of optical candidates depending on the  $\alpha_{1.4-4.85\text{GHz}}$  spectral index. We found the sources most difficult to identify to be those with ultrastep spectra and faint objects lacking the spectral-index estimates (about 35%). The fraction of unidentified objects with inverse, flat, and steep spectra is equal to 16–17%. The fraction of steep and ultrastep

---

<sup>2</sup> The RC J1131+0455 source turned out to be the gravitational lens MG J1131+0456, which was earlier identified by Hewitt et al. [37], Tonry et al. [38], and Kochanek et al. [39] using deeper images than those provided by SDSS.

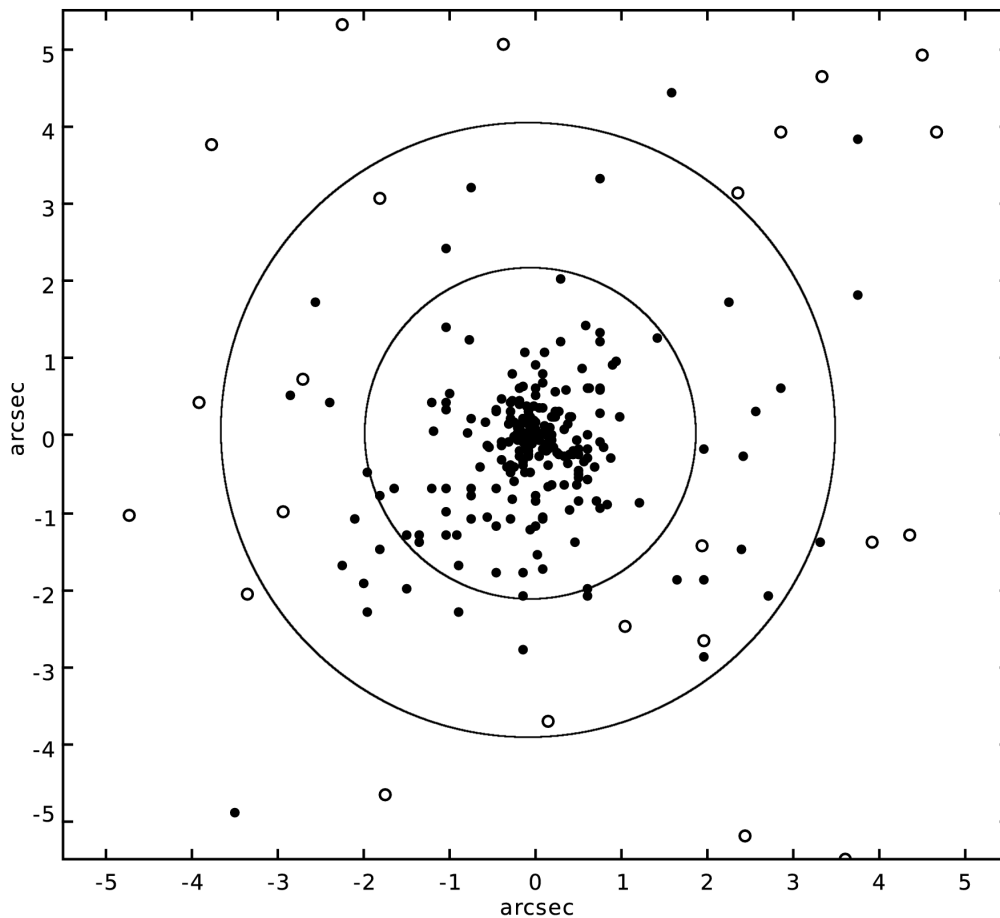


**Figure 1.** Distribution of the offset between the radio and optical coordinates for RC objects. The black dots and circles correspond to bona fide (“+”) and likely (“?”) optical identifications, respectively. The source coordinate differences in right ascension and declination are plotted along the x- and y-axis, respectively. The inner and outer circles are the boundaries of the coordinate-offset domains corresponding to  $LR_{cutoff}$  for point sources and sources with a core, respectively.

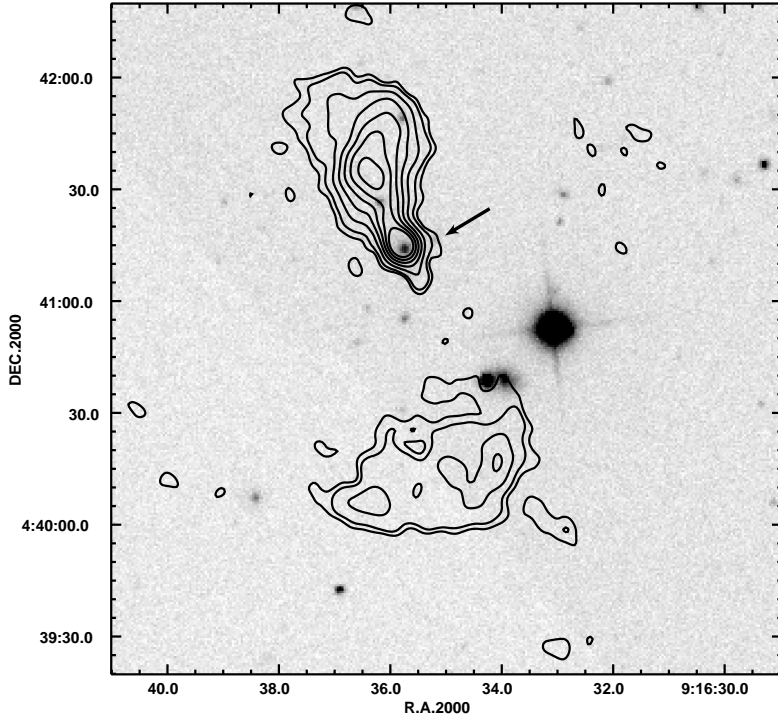
spectra is higher among the radio sources identified with galaxies than among those identified with starlike objects.

Table 3 lists the results of identification of 318 objects<sup>3</sup> depending on the morphological type of

<sup>3</sup> There are only two faint diffuse objects among the 320 radio sources, and these come from the NVSS survey. These sources are absent on the FIRST survey maps and hence cannot be identified.

the radio source. Note that double sources (D, DC, DD) were identified mostly with galaxies. The highest rate of failed identifications is among the point sources (C). The fraction of successful identifications for CJ, CL, and DC-type objects is higher and their optical counterparts are brighter than in case of point and double radio sources, and there must be more nearby objects





**Figure 2.** A composite optical (SDSS) and radio (FIRST) image of the RC J0916+0441 radio source. The isophotes drawn preserving the angular resolution show that both the Northern and Southern sources are components of a single “core-lobe” type radio source. The arrow indicates the position of the host galaxy.

among the CJ, CL, and DC-type sources. Distant objects must make up a significant fraction of unidentified double (D) and point (C) radio sources.

### 3.1. Comparison of Two Flux-Density-Complete Samples

In our first paper [34] we compare the properties of radio sources in two flux-density-complete samples of the RC catalog in the central part of the “Cold” survey. One of the samples includes 130 sources located within the  $\Delta H \leq |5'|$  strip about the center of the beam and with flux densities  $S_{3.9GHz} \geq 11$  mJy. The second sam-

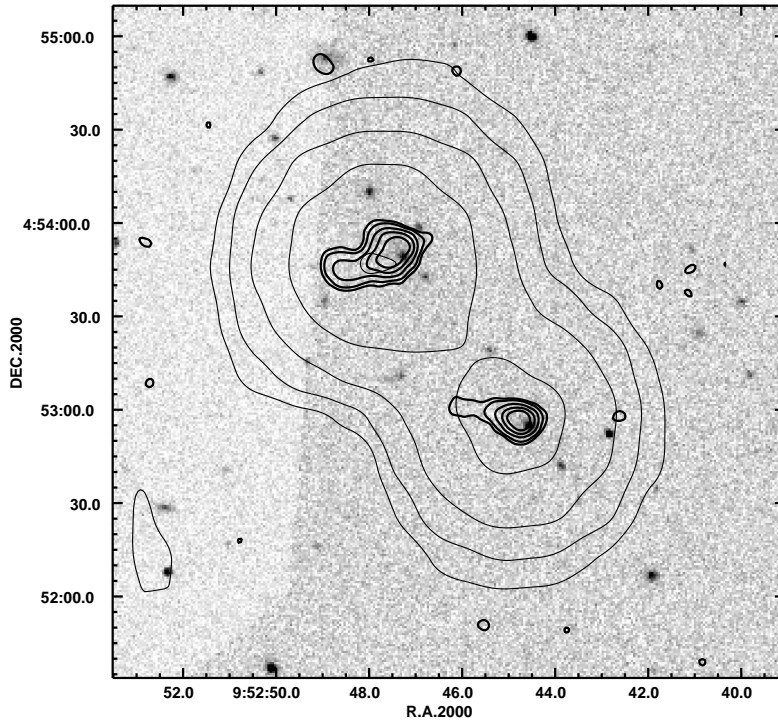
ple contains 117 sources with  $\Delta H \leq |10'|$  and  $S_{3.9GHz} \geq 30$  mJy. These samples partially overlap in terms of objects. For the sake of brevity, hereafter we refer to the first and second samples as “1S” and “2S”, respectively.

Table 4 lists the comparative results of their optical identification. The fraction of unidentified radio sources is the same in both samples.

We subdivided each sample into two groups by their 1.4–4.85 GHz spectral indices. One group includes objects with flat spectra ( $\alpha < 0.5$ ), and the other, sources with steep ( $\alpha \geq 0.5$ ) spectra. We then compared the results of identification (see Tables 5 and 6). In both samples sources with flat spectra are more

**Table 1.** The quantities that characterize the reliability of optical identification for objects of various types: the mean, root-mean-square deviation and median of the separation between the optical candidate and the radio source; the cutoff maximum-likelihood ratio, and the corresponding cutoff search radius. No data are available for four radio sources (two multicomponent objects and two objects without FIRST survey maps)

Type	$N_{obj}$	$\phi = N_+/N_{obj}$	$\Delta d_{rad-opt}^{mean}$ arcsec	$\sigma_{\Delta d_{rad-opt}}$ arcsec	$\Delta d_{rad-opt}^{med}$ arcsec	$LR_{cutoff}$	$\Delta d_{rad-opt}^{cutoff}$ arcsec
C	124 (39%)	0.64	0.94	1.30	0.47	1.79	1.88
D, DD	108 (34%)	0.72	1.43	0.87	1.26	1.93	3.49
DC, CJ, CL, T	84 (26%)	0.76	1.44	2.16	0.75	1.41	3.58



**Figure 3.** The RC J0952+0453 source is located between the two components of an NVSS source (indicated by thinner contours). The higher angular resolution of the FIRST survey allows RC J0952+0453 to be resolved into two separate radio sources, because the isophote contours are unconnected, the orientations of the major axes do not coincide, and each of the components of the radio source is identified with a separate optical object.

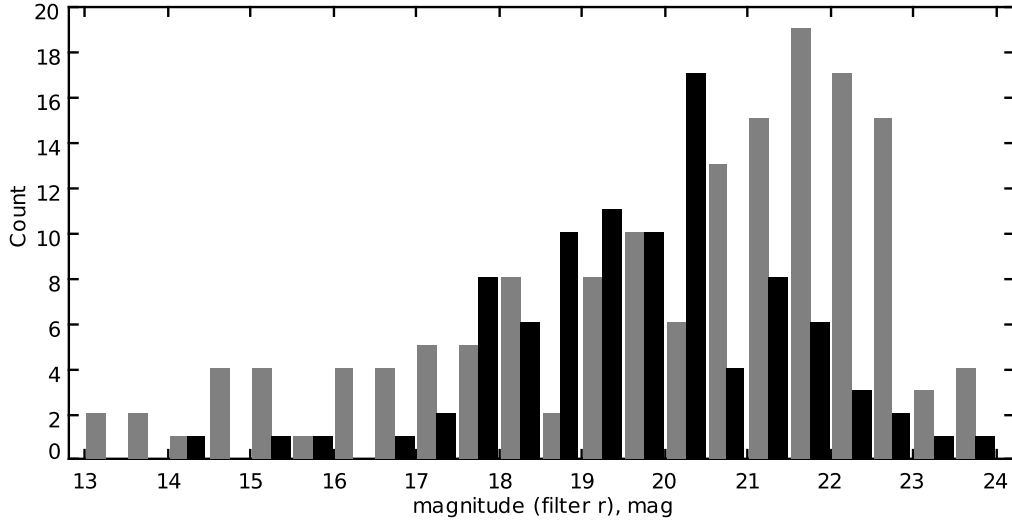


**Figure 4.** Distribution of the r-band magnitudes of optical objects identified with the RC catalog radio sources. The distributions for galaxies and stellar objects are shown by gray and black color, respectively.

**Table 2.** Results of identification depending on the  $\alpha_{1.4-4.85\text{ GHz}}$  spectral index of the radio source ( $S \sim \nu^{-\alpha}$ ) for galaxies (GALAXY), stellar objects (STAR), objects of unknown type (UNKNOWN), and unidentified sources (Empty Field or EF)

Type of identification	I ( $\alpha < -0.1$ ) (29)	F ( $-0.1 \geq \alpha < 0.5$ ) (77)	S ( $0.5 \geq \alpha < 1$ ) (142)	U ( $\alpha \geq 1$ ) (31)	Data unavailable (41)
GALAXY (157)	10	26	86	14	21
STAR (88)	14	36	28	5	6
EF (68)	5	12	25	11	14
UNKNOWN (6)	–	2	3	1	–

compact in terms of their angular sizes both in the optical domain and at radio frequencies. The sources with steep spectra are most often identified with galaxies both in the first and second samples. The fraction of identifications with starlike objects is higher for sources with flat spectra, and, moreover, the number of such objects is almost twice higher than that of galaxies in the brighter 2S sample. Starlike

objects with flat spectra form a separate group, because they differ from other objects in both samples by their color indices.

Our two samples are, according to recent radio-source counts, dominated by radio-loud AGNs. Thus most of the sources with flux densities  $S_{1.4\text{ GHz}} \geq 100\text{ mJy}$  are radio-loud AGNs with radio luminosities above  $2 \times 10^{25}\text{ WHz}^{-1}$  [40], i.e., FR II-type sources [41], whereas fainter

**Table 3.** Results of the optical identification of the objects of the RC catalog for radio sources of different morphological types. The counts do not include four sources: two multicomponent objects, which we could not attribute to any of the types mentioned below, and another two sources absent in the FIRST survey. We give the median values for LAS and  $m_r$ .

Type	$N_{obj}$	LAS, arcsec	+	?	EF	STELLAR	$m_r^{stellar}$ , mag	GALAXY	$m_r^{galaxy}$ , mag	UNKNOWN
C	123	1.4	78	10	35	39	20.23	45	21.04	4
CL	17	11.0	6	–	1	6	19.64	9	16.00	–
CJ	28	6.4	22	3	3	14	20.33	11	20.61	–
T	19	34.9	17	–	2	6	18.75	10	17.78	1
D, DC, DD	129	17.5	93	11	25	22	19.75	81	21.30	1

**Table 4.** Results of optical identification of two flux-density-complete samples (1S and 2S) in the central part of the “Cold” survey

Sample	+	?	EF	GALAXY	STAR	UNKNOWN
1S (106)	90 (70%)	16 (12%)	24 (18%)	68 (64%)	36 (34%)	2 (2%)
2S (96)	84 (72%)	12 (10%)	21 (18%)	59 (61%)	35 (36%)	2 (2%)

objects ( $1 < S_{1.4GHz} \leq 100$  mJy) are dominated by FR I-type radio sources with luminosities below the given limit [42]. The subsample of identified radio sources maintains the same galaxy-to-starlike object ratio (of about 2 : 1), despite the fact that the 1S sample is deeper in flux density terms than the 2S sample. We assume that the overwhelming majority of starlike objects are quasars as photometric and spectroscopic SDSS data suggest.

### 3.2. Redshifts of Radio Sources

Spectroscopic data are available in SDSS for 58 radio sources of our identification list. These

are 28 quasars and 30 galaxies. We found the radio sources identified with galaxies to be rather nearby objects with the median redshift and magnitude of  $Z_{galaxy}^{median} = 0.20$  and  $m_r^{median} = 18.7^m$ , respectively, whereas those identified with quasars to be distant sources ( $Z_{qsr}^{median} = 1.76$ ). The latter are brighter than galaxies by almost one magnitude ( $m_r^{median} = 17.1^m$ ). These very objects are in the group of compact radio sources with flat spectra, which we pointed out above. The most distant of the identified radio sources are quasars with redshifts  $Z > 1.7$ ; they have flat or inverse radio spectra. These are point radio sources (C) with angular sizes  $LAS \sim 2''$ , which are unresolvable in the FIRST survey.

**Table 5.** Results of optical identification of two flux-density-complete samples (1S and 2S) for flat- and steep-spectrum sources (in different intervals of  $\alpha_{1.4-4.85\text{ GHz}}$  indices)

Sample/ $N_{obj}$	Fraction, %	$S_{1.4\text{ GHz}}^{med}$ , mJy	$S_{4.85\text{ GHz}}^{med}$ , mJy	EF, %	STELLAR, %	GALAXY, %	UNKNOWN, %
1S ( $\alpha < 0.5$ ) 48	37	32.7	18	19	33	46	2
1S ( $\alpha \geq 0.5$ ) 82	63	82.3	30	18	25	56	1
2S ( $\alpha < 0.5$ ) 33	28	52.5	46	12	52	33	3
2S ( $\alpha \geq 0.5$ ) 84	72	146.5	55	20	21	69	1

**Table 6.** Results of optical identification of two flux-density-complete samples (1S and 2S) depending on the classification of objects (G – “GALAXY”; S – “STAR”) and spectral index. The columns give the median values

Sample	Type, %	$S_{4.85\text{ GHz}}$ , mJy	LAS, arcsec	$\alpha$	Size <sub>opt</sub> , arcsec	$m_u$ , mag	$m_g$ , mag	$m_r$ , mag	$m_i$ , mag	$m_z$ , mag
1S ( $\alpha < 0.5$ )	G (46)	18	2.98	0.19	1.91	22.42	21.12	20.04	19.48	19.14
	S (33)	18	2.24	0.24	1.29	21.03	20.69	20.28	19.82	19.83
1S ( $\alpha \geq 0.5$ )	G (56)	33	16.6	0.80	2.42	22.66	22.45	21.17	20.23	19.31
	S (24)	30	9.7	0.67	1.27	20.56	20.03	19.51	19.41	19.39
2S ( $\alpha < 0.5$ )	G (33)	51	1.72	0.25	1.72	22.85	19.72	18.49	18.10	17.93
	S (52)	62	2.24	0.13	1.21	21.14	20.38	19.98	19.75	19.39
2S ( $\alpha \geq 0.5$ )	G (57)	55	15.0	0.84	2.06	22.73	22.77	21.51	20.34	20.04
	S (21)	79	6.41	0.78	1.31	22.16	20.24	20.13	19.36	19.20

We gathered the data on the redshifts and apparent magnitudes of the RC catalog radio sources studied including the SS sample to analyze the redshift– $m_R$  relation (see Fig. 5). The plot is based on the data for 151 radio sources of the RC catalog: 109 galaxies and 42 quasars. These include the 58 mentioned above objects, 72 sources of the SS sample of the RC cata-

log with the redshifts measured at the 6-m telescope [23, 43–46], and 21 galaxies from among the objects identified as a result of this work. For the latter we use the photometric redshifts from the SDSS database [35], because the photometric redshifts in the  $Z_{phot} < 0.5 - 0.6$  interval for galaxies with  $m_r < 20^m$  and with redshift errors  $err_{Z_{phot}} < 0.02 - 0.03$  agree well with the empiri-

cal Z–R distribution for objects with known spectroscopic  $Z$ .

The redshift–magnitude relation<sup>4</sup> for radio galaxies shows up conspicuously out to  $Z \sim 1$  and persists at greater redshifts, whereas quasars exhibit no such relation. The Z–R diagram for radio galaxies at  $Z \geq 1.5$  forms two branches, which are possibly due to two groups of radio galaxies with different luminosities.

#### 4. COMPARISON OF TWO-FREQUENCY SPECTRAL INDICES OF RADIO GALAXIES

In the last two decades deep enough all-sky radio surveys have been conducted at various frequencies. It goes without saying that the radio loud objects at large redshifts detected in these surveys remain unidentified due to the lack of efficient methods of selecting candidate counterparts for deep objects. The use of multifrequency radio data may help to refine the radio-source selection criteria aimed at detecting distant objects.

Our list of 143 sufficiently bright sources<sup>5</sup> contains the data in the 74–4850 MHz frequency interval given from the VLSS, TXS, NVSS, and GB6 catalogs. We estimate the flux densities of some of the objects by analyzing their images in

the VLSS and GB6 surveys with the allowance for the coordinate dependent limiting sensitivity of the maps.

We compare the two-frequency spectral indices of these sources and those of the radio galaxies with  $Z > 3$  known from the literature. We took the redshifts of 33 radio galaxies with  $Z > 3$  and the flux densities at 74 and 365 MHz, 1.4 and 4.85 GHz from [45], the list of powerful radio galaxies given by Miley and De Breuck [48], and from the NED and VizieR databases.

We compare the  $\alpha_{74-365\text{ MHz}}$  and  $\alpha_{365-1400\text{ MHz}}$ ;  $\alpha_{365-1400\text{ MHz}}$  and  $\alpha_{1.4-4.85\text{ GHz}}$ , as well as  $\alpha_{74-365\text{ MHz}}$  and  $\alpha_{1.4-4.85\text{ GHz}}$  spectral indices for the RC-catalog radio sources and radio galaxies with redshifts  $Z > 3$  studied in this paper. Figure 6 shows by way of an example a comparison of spectral indices. Two-frequency spectral indices for radio galaxies with large redshifts differ from the corresponding indices for most of our sources. Thus radio galaxies with  $Z > 3$  fall within the region determined by the following constraints on spectral indices:

- $\alpha_{74-365\text{ MHz}} > 0.5$ ;
- $\alpha_{365-1400\text{ MHz}} > 0.9$ ;
- $\alpha_{1.4-4.85\text{ GHz}} > 0.7$ .

We selected from our list 18 radio sources with spectral indices fall within the same area as the spectral indices of galaxies with large redshifts. Thirteen of these sources appear in the SS sample of the RC catalog. Nine of

<sup>4</sup> We transform  $m_r$  into  $m_{R_c}$  by the formula from Jordi et al. [47].

<sup>5</sup> We give for these sources the median flux densities at the following frequencies:  $S_{74\text{ MHz}}=1070\text{ mJy}$ ,  $S_{365\text{ MHz}}=450\text{ mJy}$ ,  $S_{1.4\text{ GHz}}=75\text{ mJy}$ ,  $S_{4.85\text{ GHz}}=41\text{ mJy}$ .

these 18 sources have their redshifts measured by the spectroscopic data obtained with the 6-m telescope of the Special Astrophysical Observatory of the Russian Academy of Sciences [46]. Their median magnitudes, angular sizes, and redshifts are equal to  $m_R = 22.6^m$ ,  $LAS = 20.1''$ , and  $Z=0.82$ , respectively. No redshifts are known for the remaining nine objects, which are fainter than  $m_R^{median} = 23.4^m$  and have smaller angular sizes ( $LAS^{median} = 7.6''$ ): RC J0820+0454, RC J0945+0454, RC J1347+0441, RC J1439+0455 (these sources are in the SS sample of the RC catalog) and RC J1251+0446, RC J1357+0507, RC 1434+0445, RC J1456+0456, and RC J1607+0438. The empirical Z–R relation for the RC catalog (Fig. 5) allows the redshifts of these objects to be estimated as  $Z \geq 1.5$ . Their small angular sizes are consistent with this estimate, however, only spectroscopic observations may finally confirm our hypotheses.

## 5. CONCLUSIONS

The software for the analysis and visualization of observational data developed in the past decade, and free access to modern surveys offer new, hitherto unavailable opportunities for the study of celestial objects. At the same time, the new tools impose new requirements both on the formulation of the problems and on the methods of investigation, which in technological solutions are increasingly dependent on information

technologies and, first and foremost, on database management systems and web services.

Mass identification of sources from various surveys and catalogs is of real interest for the astronomers. Automating the identification process by using already operational virtual observatory web services, which appears to be rather easy to implement, is still far from perfect. This especially concerns the radio data because of the wide range of angular resolution, limiting sensitivity, coordinate accuracy of the catalogs, and the nature of radio sources.

The coordinate accuracy of the NVSS and FIRST surveys allows them to be automatically cross-identified with optical surveys. A number of authors report the results of identification with the APM [49] and SDSS [50] optical surveys. The resulting rate of successful identifications is rather low. It was equal to 24% and 27% in the former and latter cases, respectively. If the coordinate accuracy of the catalog is lower than that of the NVSS and SDSS surveys, as, e.g., in GB6, the rate of successful identifications is even lower—of about 0.2% [51]. The number of FIRST sources identified with SDSS is about 30–40% of all objects in the catalog. These are single-component sources with the offset between the optical and radio coordinates no greater than  $2''$ .

Cross-identification services operate by the simple algorithm searching for the nearest object to the center of the given region. This algorithm efficiently identifies single-component

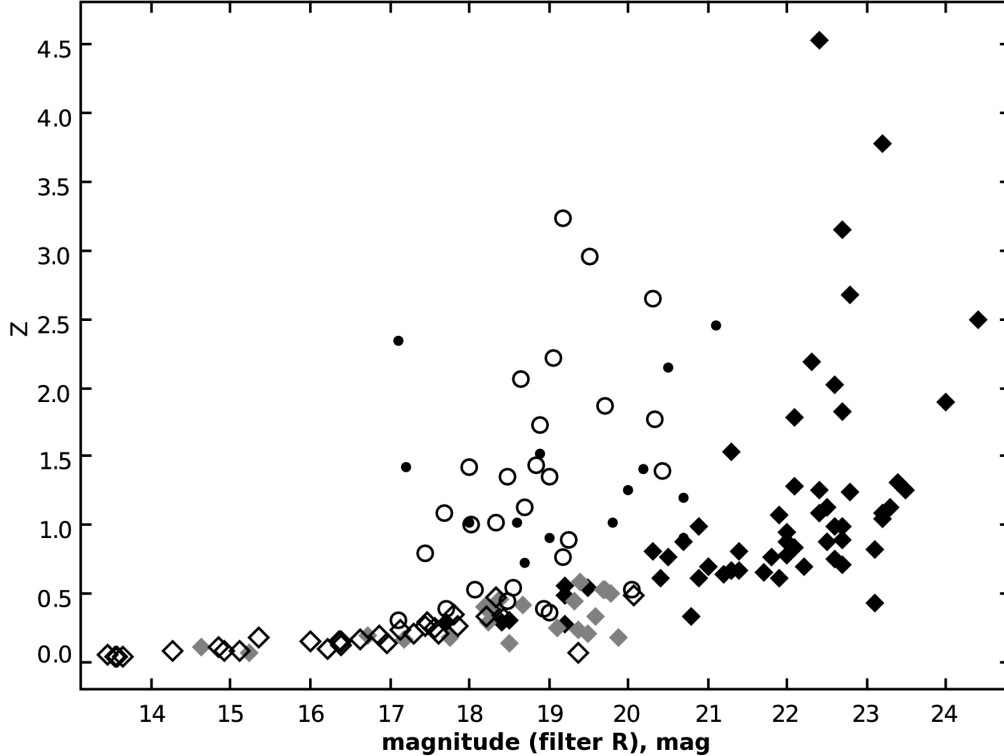


**Figure 5.** The  $m_R$  magnitude–redshift relation for the radio sources of the RC catalog. The diamond signs and circles correspond to the galaxies and quasars, respectively (the filled diamond signs and circles indicate the redshifts  $Z$  measured at the 6-m telescope, and the redshifts of the objects shown by other symbols are adopted from the SDSS database).

radio sources, but handles poorly sources with more complex structure. The efficiency of optical identification of radio sources delivered by the existing cross-identification algorithms does not exceed 30%.

We decided to analyze the RC-catalog sample in order to understand to which extent automatic identification of radio sources can be performed in case where the angular resolution and coordinate accuracy of the catalog are insufficient for optical identification, what fraction of sources can be identified, and to find out the problems

and restrictions of such a procedure.

Due to the insufficient coordinate accuracy of the RC catalog the procedure of identification of the sample in the area overlapping with the SDSS and FIRST surveys consists of two stages. We first refined the coordinates of the radio sources of the catalog by cross-identifying them with the sources in other radio catalogs with better coordinate accuracy (mostly NVSS, which we used as our reference catalog). In the doubtful cases we used not only the data from the catalogs, but also the images provided in the radio surveys. We



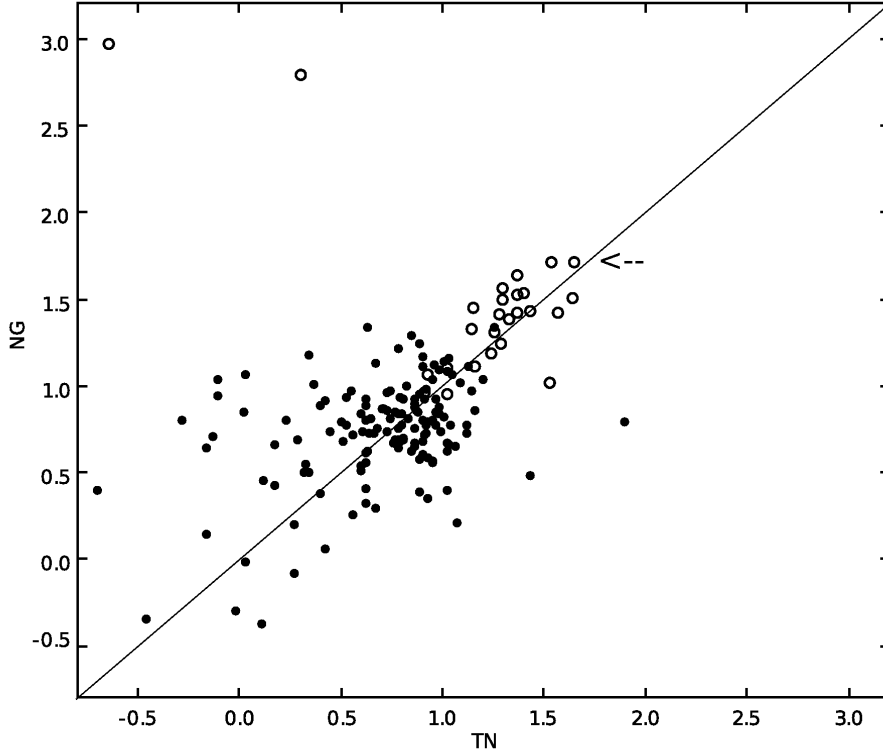


**Figure 6.** Comparison of two-frequency spectral indices  $\alpha_{365-1400\text{ MHz}}$  (TN) and  $\alpha_{1.4-4.85\text{ GHz}}$  (NG) for 143 bright sources from the list studied (filled circles) and for known distant radio galaxies with  $Z > 3$  (open circles). Also shown is the equal-index line. The arrow indicates the most distant known radio galaxy ( $Z = 5.2$ ).

performed optical identification using refined radio coordinates and contour radio maps based on the FIRST survey images. We refined the classification of sources for it to include seven types, because we concluded that the classification including FRI, FRII, and point sources failed to fully reflect the structural variety of the sources of the FIRST survey.

We identified 320 radio sources of the RC catalog with sources from other radio catalogs and with optical objects. We measured the angular sizes of these objects and counted the number of their components listed in the FIRST catalog. We found the ratio of the radio sources with

one-, two-, three-, and four or more components to be of about 10:5:2:1.

It follows from these counts that simple cross-identification algorithms (based on the nearest neighbor search) are the most efficient ones for single-component sources (56% of the list) provided the optical survey is deep enough. The algorithms must be modified if they are going to be used for identifying double sources, which make up for about one third of the list. One fifth of the list can be identified by inspecting optical and radio images or by applying cross-identification algorithms involving elements of pattern recognition. We identified our sample with SDSS and

found optical candidates for about 75% of single-component sources, which make up for 33% of the entire list.

Cross-identification depends essentially on the adopted search radius, which is a parameter characterizing the two catalogs compared. Thus the optimum search radius for FIRST and SDSS catalogs for single-component sources is  $2''$ . Identification is unlikely if the the separation between the radio source and optical object is greater than this radius.

We compared the threshold values for the maximum-likelihood ratio functions for three groups of sources in our sample—point, double, and non-point sources with the coincident positions of the optical object and radio-emission peak, to obtain our own estimate for the search region for optical objects in the FIRST survey. The search radius for point sources is of about  $1.9''$ , which almost coincides with the search radius for FIRST and SDSS mentioned above. The search radius for non-point and double sources is of about  $3.6''$  if the search region center is set to coincide with the center of the radio source as we define it in our first paper [34].

We found candidate optical identifications for almost 80% of the radio sources of the list studied and no candidates for the remaining 20% of the sources, i.e., optical objects proved to be fainter than the limiting magnitude of the SDSS survey ( $r = 22.6^m$ ). The galaxy-to-starlike object ratio among identified sources is of about 2 : 1, and starlike objects are most probably quasars judg-

ing by the photometric and spectroscopic SDSS data.

The distribution of the results of identifications by morphological type of the radio source is such that most of the optical candidates have been found for CJ, CL, and T-type sources; smaller amount of optical candidates could be found for double radio sources, and even less for point sources. Double sources are mostly identified with galaxies. CL and T-type sources are identified with brighter optical objects than CJ-type, double, and point radio sources. A large fraction of radio sources identified with galaxies have steep and ultrastep spectra in the 1.4–4.85 GHz frequency interval compared to starlike objects, however, the fraction of objects with steep and ultrastep spectra is even higher among the radio sources in “empty fields”. Some of the unidentified point sources and objects with ultrastep spectra in the 1.4–4.85 GHz frequency interval may have large  $Z$ .

The structure of a radio source may bear information about recurrent phases of its activity in the host galaxy. Such systems include “winged” or “X-shaped” radio sources [52, 53], “double-double” radio galaxies [54], and triple sources (T) with two components straddling relatively bright, unresolved cores [55]. According to FIRST survey maps, about 12 – 17% of the radio sources of the sample studied can be classified as “X-shaped”, “double-double”, or triple, i.e., as sources with recurrent activity phases.

We analyzed the physical parameters of the

identified radio sources by comparing two flux-density-complete samples from the central part of the survey [34]: one with  $S_{3.9\text{MHz}}^{\text{lim}} \geq 10$  mJy and another with  $S_{3.9\text{MHz}}^{\text{lim}} \geq 30$  mJy. We found the fraction of unidentified radio sources to be the same in both samples, and the galaxy-to-starlike object ratio to be the same (of about 2:1) in both subsamples of identified sources. However, the two samples differ in the fraction of sources with flat and steep spectra. The deeper sample contains more objects with flat and inverse spectra and less objects with steep and ultrasteep spectra.

In both samples sources with flat spectra are more compact in terms of angular size both on optical and radio images. Steep-spectrum sources are more often identified with galaxies, and flat-spectrum sources—with starlike objects. Note that in the 2S sample the number of identifications of flat-spectrum sources with starlike objects is almost twice the number of identifications with galaxies. In both samples starlike objects with flat spectra differ in color from the galaxies with flat spectra, whereas no such differences are observed for sources with steep spectra.

Optical identification with SDSS revealed a group of nearby radio galaxies with  $Z_{\text{sp}}^{\text{median}}=0.20$  and  $m_r^{\text{median}} = 18.7^m$  and a group of rather distant radio-loud quasars with  $Z_{\text{sp}}^{\text{median}}=1.76$ ,  $m_r^{\text{median}} = 17.1^m$ . Note that quasars with  $Z > 1.7$  are point sources with angular sizes  $LAS^{\text{median}} \sim 2''$ . Quasars have flat and inverse radio spectra and, possibly, make up

the above-mentioned group of radio sources with flat spectra and with a spectral distribution that is different from that of other sources.

The steepness of the spectrum of a radio source from low to high frequencies is widely used as a criterion for selecting possible distant objects. We compared the spectral indices for the sources in our list, for those with the data at 74, 365 MHz and 1.4, 4.85 GHz are available, with 33 known radio galaxies with  $Z > 3$ . We found that distant objects occupy a certain region of index values on two-frequency indices plots. We selected from the list studied the radio sources with spectral indices fall within the same region as the spectral indices of galaxies at large redshifts. Two thirds of these sources belong to the SS sample of the RC catalog and most of them have their redshifts measured ( $Z^{\text{median}}=0.82$ ) [46], whereas objects with unknown  $Z$  are fainter and have smaller angular sizes. The last group in terms of apparent magnitude occupies the domain of RC catalog sources with  $Z \geq 1.5$  on the  $Z$ -R diagram (Fig. 5), i.e., these objects are most likely rather distant galaxies. A comparison of the spectral indices of the sources studied with those of distant galaxies led us to conclude that the shape of the radio spectrum in the 74–4850 MHz interval provides additional information that may help to refine the choice of candidate distant objects.

The tables with the results of the optical cross-identification of 320 radio sources of the RC catalog with SDSS, USNO-B1, and 2MASS are available in electronic

form along with their description from  
<http://www.sao.ru/hq/zhe/RCoiRes.html>.

## ACKNOWLEDGMENTS

The large amount and inhomogeneous nature of the data, which includes eight catalogs and four surveys, would be impossible to pre-

pare and analyze without new software tools developed in accordance with IVOA standards, namely Aladin [29], Vizier [56], TOPCAT [57], and CasJobs [58].

This work was supported by the Russian Foundation for Basic Research (grant No 06-07-08062).

- 
- |  |  |
|--|--|
| 1. \refitem{ <i>article</i> }  | 10. \refitem{ <i>misc</i> }  |
| A.S. Bennet, Mem.RAS. <b>68</b> , 163 (1962).  | J.K. Katgert et al., IAU Symp. <b>74</b> , 165 (1977).                               |
| 2. \refitem{ <i>article</i> }  | 11. \refitem{ <i>misc</i> }  |
| R.A. Laing et al., Monthly Notices Roy. Astronom. Soc. <b>204</b> , 151 (1983).          | @ M. Irwin and R. McMahon, IAU Comm. <b>9</b> Newletters <b>2</b> , 31 (1992).       |
| 3. \refitem{ <i>article</i> }  | 12. \refitem{ <i>article</i> }   |
| J. Kristian et al., Astrophys. J. <b>191</b> , 43 (1974).                                | D.G. Monet et al., Astronom. J. <b>125</b> , 984 (2003).                             |
| 4. \refitem{ <i>article</i> }  | 13. \refitem{ <i>article</i> }   |
| G.G. Pooley et al., Monthly Notices Roy. Astronom. Soc. <b>224</b> , 847 (1987).         | J.E. Morrison et al., Astronom. J. <b>121</b> , 3, 1752 (2001).                      |
| 5. \refitem{ <i>article</i> }  | 14. \refitem{ <i>article</i> }   |
| S. Rawlings et al., Monthly Notices Roy. Astronom. Soc. <b>279</b> , L13 (1996).         | A.B.Berlin et al., Pis'ma Astron. Zh. <b>7</b> , 290 (1981).                         |
| 6. \refitem{ <i>article</i> }  | 15. \refitem{ <i>article</i> }   |
| S. de Koff et al., Astrophys. J. Suppl. <b>107</b> , 621 (1996).                         | A.B.Berlin et al., Pis'ma Astron. Zh. <b>9</b> , 211 (1983).                         |
| 7. \refitem{ <i>article</i> }  | 16. \refitem{ <i>article</i> }   |
| M P.J. McCarthy et al., Astrophys. J. Suppl. <b>112</b> , 415 (1997).                    | Yu.N. Pariiskij et al., Astronom. and Astrophys. Suppl. Ser. <b>87</b> , 1 (1991).   |
| 8. \refitem{ <i>article</i> }  | 17. \refitem{ <i>article</i> }   |
| A.R. Martel et al., Astronom. J. <b>115</b> , 1348 (1998).                               | Yu.N. Parijskij et al., Astronom. and Astrophys. Suppl. Ser. <b>96</b> , 583 (1992). |
| 9. \refitem{ <i>article</i> }  | 18. \refitem{ <i>article</i> }   |
| G. Grueff and M. Vigotti M., Astronom. and Astrophys. Suppl. Ser. <b>20</b> , 57 (1975). | V.V. Vitkovskij et al., Soobschenija SAO   |

- 53**, 86 (1987).
19. \refitem{*article*}  
J.N. Douglas et al., *Astronom. J.* **111**, 1945 (1996).
  20. \refitem{*article*}  
N.S. Soboleva et al., *Astron. Zh.* **71**, 684 (1994).
  21. \refitem{*article*}  
A. Fletcher et al., *Astronomy Reports* **40**, 759 (1996).
  22. \refitem{*article*}  
A.I. Kopylov, *Astron. Zh.* **72**, 437 (1995).
  23. \refitem{*article*}  
Yu.N. Parijskij et al., *BSAO* **40**, 5 (1996).
  24. \refitem{*article*}  
O.V. Verkhodanov et al., *BSAO* **52**, 3 (2001).
  25. \refitem{*misc*}  
B.M. Lasker et al., *ASP Conf. Ser.* **101**, 88 (1996).
  26. \refitem{*article*}  
K. Abazajian et al., *Astronom. J.* **129**, 1755 (2005).
  27. \refitem{*article*}  
R.H. Becker et al., *Astrophys. J.* **475**, 479 (1997).
  28. \refitem{*article*}  
J.J. Condon et al., *Astronom. J.* **115**, 1693 (1998).
  29. \refitem{*article*}  
F. Bonnarel et al., *Astronom. and Astrophys. Suppl. Ser.* **143**, 33 (2000).
  30. \refitem{*misc*}  
FIRST cutout service,  
<http://www.mrao.cam.ac.uk/surveys/FIRST/>.
  31. \refitem{*article*}  
C.R. Lawrence et al., *Astrophys. J. Suppl.* **61**, 105 (1986).
  32. \refitem{*article*}  
P.N. Best et al., *Monthly Notices Roy. Astronom. Soc.* **346**, 627 (2003).
  33. \refitem{*misc*}  
R.M. Cutri et al., *The 2MASS all-Sky Catalog of Point Sources* (2003).
  34. \refitem{*article*}  
O.P. Zhelenkova and Kopylov A.I., *Astroph. Bull.* **63**, 369 (2008).
  35. \refitem{*article*}  
I. Csabai et al., *Astronom. J.* **125**, 580 (2003).
  36. \refitem{*article*}  
Collister, Lahav, *Publ. Astronom. Soc. Pacific* **116**, 818, 345 (2004).
  37. \refitem{*article*}  
J.H. Hewitt et al., *Nature* **333**, 537 (1988).
  38. \refitem{*article*}  
J.L. Tonry et al., *Astronom. J.* **119**, 1078 (2000).
  39. \refitem{*article*}  
C.S. Kochanek et al., *Astrophys. J.* **535**, 692 (2000).
  40. \refitem{*article*}  
C.J. Willott et al., *Monthly Notices Roy. Astronom. Soc.* **335**, 1120 (2002).
  41. \refitem{*article*}  
B.L. Fanaroff and Riley, J.M., *Monthly Notices Roy. Astronom. Soc.* **167**, 31P (1974).
  42. \refitem{*article*}  
R.A. Windhorst et al., *Astrophys. J.* **289**, 494 (1985).
  43. \refitem{*article*}  
V.L. Afanasev et al., *Astronomy Reports* **47**, 377 (2003).
  44. \refitem{*article*}  
N.S. Soboleva et al., *Astron. Lett.* **26**, 623

- (2000).
45. \refitem{*article*}  
A.I. Kopylov et al., Pis'ma Astron. Zh. **32**, 433 (2006).
46. \refitem{*misc*}  
A.I. Kopylov, priv. (2007)
47. \refitem{*article*}  
K. Jordi et al., Astronom. and Astrophys. **460**, 339 (2006).
48. \refitem{*article*}  
G. Miley and De Breuck,C., arXiv:0802.2770 (2008).
49. \refitem{*article*}  
R.G. McMahon et al., Astrophys. J. Suppl. **143**, 1 (2002).
50. \refitem{*article*}  
Ž. Ivezić et al., Astronom. J. **124**, 2364 (2002).
51. \refitem{*article*}  
M. Obrić et al., Monthly Notices Roy. Astronom. Soc. **370**, 1677 (2006).
52. \refitem{*article*}  
F.K. Liu, Monthly Notices Roy. Astronom. Soc. **347**, 1357 (2004).
53. \refitem{*article*}  
C.C. Cheung, Astronom. J. **133**, 2097 (2007).
54. \refitem{*article*}  
L. Lara et al., Astronom. and Astrophys. **348**, 699 (1999).
55. \refitem{*article*}  
A. Marecki et al., Astronom. and Astrophys. **448**, 479 (2006).
56. \refitem{*article*}  
F. Ochsenbein et al., Astronom. and Astrophys. Suppl. Ser. **143**, 221 (2000).
57. \refitem{*misc*}  
M.B. Taylor, ASP Conf. Series **347**, 29 (2005).
58. \refitem{*misc*}  
A.R. Thakar et al., ASP Conf. Series **347**, 684 (2005).